

# Parametric Space for Elastic Waves in Porous Media with Complex Rheology

Adham A. Ali

Department of Mathematics, Kirkuk University, Kirkuk, Iraq  
 Email: Adham.ali@uokirkuk.edu.iq

Dmitry V. Strunin

School of Sciences, University of Southern Queensland, Toowoomba, Australia  
 Email: strunin@usq.edu.au

**Abstract**—We evaluate the influence of mechanical parameters on the decay rate of elastic waves in fluid-saturated media with bubbles. The parameters describe the complex rheological scheme adopted as a model of the grainy porous medium. Areas of validity of the model in the space of mechanical parameters are determined.

**Index Terms**—elastic waves, rheology, decay rate, parameters

## I. INTRODUCTION

Wave propagation in fluid-saturated porous media attracts constant attention of researchers and engineers due to the many applications in geomechanics, oil extraction industry and because of theoretical significance [1]-[7]. Recently we used [8] an extended rheological model relative to the earlier model of Nikolaevskiy [9, 10], to study the influence of the bubbles on the linear Frenkel–Biot waves of P1 type. The rheological model for the wave with the bubbles, shown in Fig. 1, consists of three segments representing the solid continuum, fluid continuum and a bubble surrounded by the fluid. Based on the rheological model, we derived, using the procedure similar to [10], the one-dimensional partial differential equation for the nonlinear longitudinal seismic wave,

$$C_1 \frac{\partial v}{\partial \tau} - C_2 \frac{\partial^2 v}{\partial \xi^2} + \varepsilon C_3 \frac{\partial^3 v}{\partial \xi^3} - \varepsilon^2 C_4 \frac{\partial^4 v}{\partial \xi^4} - \varepsilon^4 C_6 \frac{\partial^6 v}{\partial \xi^6} - C_7 \frac{\partial v v}{\partial \xi} = 0, \quad (1)$$

where  $v$  is the velocity of the solid matrix,  $\varepsilon$  is the small parameter responsible for slow behaviour of the wave in space and time, and the coefficients  $C_i, i=1, 2, 3, 4, 6, 7$  are constants linked to the mechanical parameters of the system. From (1) follows the dispersion relation

$$\lambda(k) = -\frac{C_2}{C_1} k^2 + \varepsilon^2 \frac{C_4}{C_1} k^4 - \varepsilon^4 \frac{C_6}{C_1} k^6, \quad (2)$$

Describing the behavior of the wave in time,  $v \sim \exp(\lambda t)$ ;  $k$  is the wave number. We discovered [8] that the increase of the radius of the bubbles,  $R_0$ , leads to faster decay, while the increase of the number of the bubbles,  $n_0$ , leads to slower decay of the wave as shown in Fig 2.

The aim of this paper is to evaluate the ranges of the parameters of the rheological model that lead to negative values of  $\lambda$ , which describe a *decaying* wave and are, therefore, physically acceptable (valid), and to positive  $\lambda$  which describe a *growing* wave, and are, therefore, physically not acceptable (invalid). In this paper we use  $k = 0.25$  1/m,  $\varepsilon = 0.01$  [8].

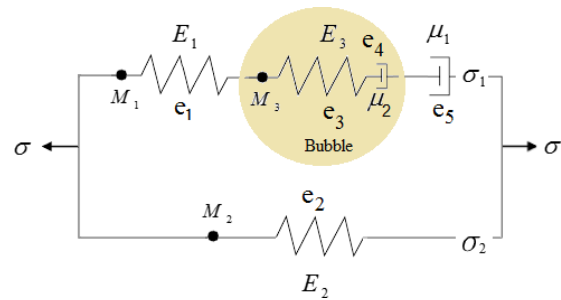


Figure 1. Rheological scheme including a gas bubble [8].

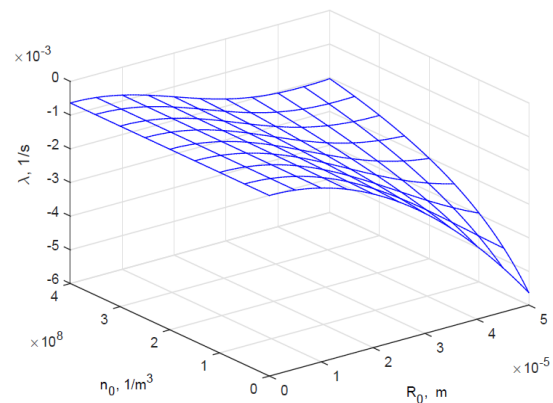


Figure 2. The decay rate  $\lambda$  versus  $R_0$  and  $n_0$ , from [8].

II. RHEOLOGICAL PARAMETERS

In this section we focus on the parameters of the rheological model shown in Fig. 1. The model includes two friction elements with viscosities  $\mu_1$  and  $\mu_2$ , three elastic springs with the elastic moduli  $E_1$ ,  $E_2$ , and  $E_3$ , and three oscillating masses  $M_1$ ,  $M_2$ , and  $M_3$ . Further,  $\sigma$  is the total stress;  $e$  with respective subscript denotes the displacement of the element of the model. Overall we have 8 independent rheological parameters,  $E_1, E_2, E_3, M_1, M_2, M_3, \mu_1$  and  $\mu_2$ . The magnitudes of the viscosities  $\mu_1$  and  $\mu_2$  are well known from literature [11, 12] while the parameters  $E_1, E_2, E_3, M_1, M_2$  and  $M_3$  are known quite poorly and only be roughly estimated by the order of magnitude. We aim to determine a possibly wider range of the values of the parameters making the decay rate negative (valid).

As for the values of  $E_i$  and  $M_i$ , they are roughly suggested in [10, 13, 14, 15], and we let them vary from these reference levels by a few orders of magnitude. Tables I and II show the values for  $E_i$  and  $M_i$  which we use in the present study.

TABLE I. THE VALUES OF  $E_1, E_2$  AND  $E_3$

	$E_1, \text{Pa}$	$E_2, \text{Pa}$	$E_3, \text{Pa}$
1	$10^4$	$10^5$	$10^2$
2	$10^5$	$10^6$	$5 \times 10^2$
3	$10^6$	$10^7$	$10^3$

TABLE II. THE VALUES OF  $M_1, M_2$  AND  $M_3$

	$M_1, \text{Kg/m}$	$M_2, \text{Kg/m}$	$M_3, \text{Kg/m}$
1	$10^{-2}$	$5 \times 10^{-2}$	$5 \times 10^{-5}$
2	$10^{-3}$	$5 \times 10^{-3}$	$5 \times 10^{-6}$
3	$10^{-4}$	$5 \times 10^{-4}$	$5 \times 10^{-7}$

Tables I and II give  $3^3 \times 3^3 = 27 \times 27$  possible combinations of the parameter values. In order to reduce the amount of calculations, for each of the 27 combinations of  $E_i$  from Table I we consider only one combination of  $M_i$  from Table II, namely one with the same row and column number, see Table III. For each row from Table III, we plot the decay rate against the radius of the bubbles,  $R_0$ , and their number (concentration),  $n_0$ . In total Table III gives 27 possible graphs, but some of these graphs are very close as we comment in the figure captions. The results are presented in Figs. 3-5.

We found the following. When the values of  $E_1$  and  $E_3$  are simultaneously increased to  $10^{12}$  Pa the decay rate  $\lambda$  remains negative (valid). When they are simultaneously decreased down to  $10^2$  Pa the decay rate  $\lambda$  gets less negative. With the increase of the value of  $E_2$  to  $6 \times 10^9$  Pa the decay rate  $\lambda$  becomes positive (invalid), see Figs. 6 and 7. This indicates that our model is not applicable to such extreme values of  $E_2$ .

TABLE III. THE VALUES OF  $E_1, E_2, E_3, M_1, M_2$  AND  $M_3$ , CONSIDERED IN THIS PAPER

	$E_1, \text{Pa}$	$E_2, \text{Pa}$	$E_3, \text{Pa}$	$M_1, \text{Kg/m}$	$M_2, \text{Kg/m}$	$M_3, \text{Kg/m}$
1	$10^4$	$10^5$	$10^2$	$10^{-2}$	$5 \times 10^{-2}$	$5 \times 10^{-5}$
2	$10^4$	$10^5$	$5 \times 10^2$	$10^{-2}$	$5 \times 10^{-2}$	$5 \times 10^{-6}$
3	$10^4$	$10^5$	$10^3$	$10^{-2}$	$5 \times 10^{-2}$	$5 \times 10^{-7}$
4	$10^4$	$10^6$	$10^2$	$10^{-2}$	$5 \times 10^{-3}$	$5 \times 10^{-5}$
5	$10^4$	$10^6$	$5 \times 10^2$	$10^{-2}$	$5 \times 10^{-3}$	$5 \times 10^{-6}$
6	$10^4$	$10^6$	$10^3$	$10^{-2}$	$5 \times 10^{-3}$	$5 \times 10^{-7}$
7	$10^4$	$10^7$	$10^2$	$10^{-2}$	$5 \times 10^{-4}$	$5 \times 10^{-5}$
8	$10^4$	$10^7$	$5 \times 10^2$	$10^{-2}$	$5 \times 10^{-4}$	$5 \times 10^{-6}$
9	$10^4$	$10^7$	$10^3$	$10^{-2}$	$5 \times 10^{-4}$	$5 \times 10^{-7}$
10	$10^5$	$10^5$	$10^2$	$10^{-3}$	$5 \times 10^{-2}$	$5 \times 10^{-5}$
11	$10^5$	$10^5$	$5 \times 10^2$	$10^{-3}$	$5 \times 10^{-2}$	$5 \times 10^{-6}$
12	$10^5$	$10^5$	$10^3$	$10^{-3}$	$5 \times 10^{-2}$	$5 \times 10^{-7}$
13	$10^5$	$10^6$	$10^2$	$10^{-3}$	$5 \times 10^{-3}$	$5 \times 10^{-5}$
14	$10^5$	$10^6$	$5 \times 10^2$	$10^{-3}$	$5 \times 10^{-3}$	$5 \times 10^{-6}$
15	$10^5$	$10^6$	$10^3$	$10^{-3}$	$5 \times 10^{-3}$	$5 \times 10^{-7}$
16	$10^5$	$10^7$	$10^2$	$10^{-3}$	$5 \times 10^{-4}$	$5 \times 10^{-5}$
17	$10^5$	$10^7$	$5 \times 10^2$	$10^{-3}$	$5 \times 10^{-4}$	$5 \times 10^{-6}$
18	$10^5$	$10^7$	$10^3$	$10^{-3}$	$5 \times 10^{-4}$	$5 \times 10^{-7}$
19	$10^6$	$10^5$	$10^2$	$10^{-4}$	$5 \times 10^{-2}$	$5 \times 10^{-5}$
20	$10^6$	$10^5$	$5 \times 10^2$	$10^{-4}$	$5 \times 10^{-2}$	$5 \times 10^{-6}$
21	$10^6$	$10^5$	$10^3$	$10^{-4}$	$5 \times 10^{-2}$	$5 \times 10^{-7}$
22	$10^6$	$10^6$	$10^2$	$10^{-4}$	$5 \times 10^{-3}$	$5 \times 10^{-5}$
23	$10^6$	$10^6$	$5 \times 10^2$	$10^{-4}$	$5 \times 10^{-3}$	$5 \times 10^{-6}$
24	$10^6$	$10^6$	$10^3$	$10^{-4}$	$5 \times 10^{-3}$	$5 \times 10^{-7}$
25	$10^6$	$10^7$	$10^2$	$10^{-4}$	$5 \times 10^{-4}$	$5 \times 10^{-5}$
26	$10^6$	$10^7$	$5 \times 10^2$	$10^{-4}$	$5 \times 10^{-4}$	$5 \times 10^{-6}$
27	$10^6$	$10^7$	$10^3$	$10^{-4}$	$5 \times 10^{-4}$	$5 \times 10^{-7}$

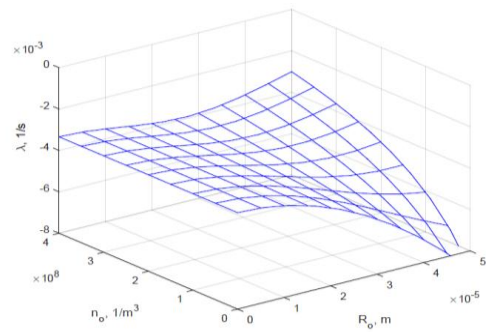


Figure 3. The decay rate by formula (2) for row 1 of Table III.

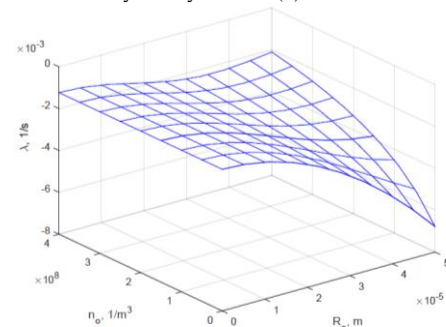


Figure 4. The decay rate by formula (2) for row 11 of Table III.

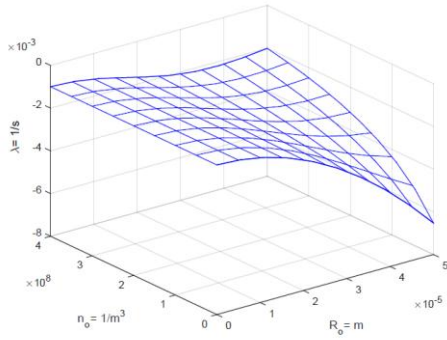


Figure 5. The decay rate by formula (2) for row 27 of Table III.

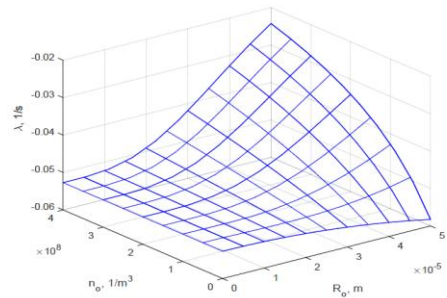


Figure 6. The decay rate by formula (2) for  $E_1, E_3=10^2$  Pa.

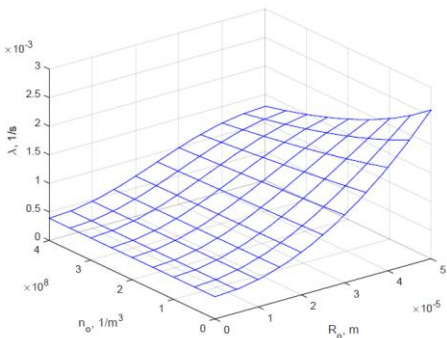


Figure 7. The decay rate by formula (2) for  $E_2=6 \times 10^9$  Pa.

All the presented calculations are carried out for the number of bubbles  $n_0 = 10^8 \text{ 1/m}^3$  and the radius of bubbles  $R_0 = 5 \times 10^{-5} \text{ m}$  [8, 16]. Similar results are obtained when possible values of  $E_i$  are extended as shown in Table IV. Figs. 8-10 show the results for the parameter values given in Table IV.

TABLE IV. THE VALUES OF  $E_1, E_2$  AND  $E_3$

	$E_1, \text{Pa}$	$E_2, \text{Pa}$	$E_3, \text{Pa}$
1	$10^9$	$5 \times 10^7$	$10^6$
2	$10^9$	$5 \times 10^7$	$5 \times 10^6$
3	$10^9$	$5 \times 10^7$	$8 \times 10^7$
4	$10^9$	$10^8$	$10^6$
5	$10^9$	$10^8$	$5 \times 10^6$
6	$10^9$	$10^8$	$8 \times 10^7$
7	$10^9$	$4 \times 10^9$	$10^6$
8	$10^9$	$4 \times 10^9$	$5 \times 10^6$
9	$10^9$	$4 \times 10^9$	$8 \times 10^7$
10	$5 \times 10^9$	$5 \times 10^7$	$10^6$

11	$5 \times 10^9$	$5 \times 10^7$	$5 \times 10^6$
12	$5 \times 10^9$	$5 \times 10^7$	$8 \times 10^7$
13	$5 \times 10^9$	$10^8$	$10^6$
14	$5 \times 10^9$	$10^8$	$5 \times 10^6$
15	$5 \times 10^9$	$10^8$	$8 \times 10^7$
16	$5 \times 10^9$	$4 \times 10^9$	$10^6$
17	$5 \times 10^9$	$4 \times 10^9$	$5 \times 10^6$
18	$5 \times 10^9$	$4 \times 10^9$	$8 \times 10^7$
19	$10^{10}$	$5 \times 10^7$	$10^6$
20	$10^{10}$	$5 \times 10^7$	$5 \times 10^6$
21	$10^{10}$	$5 \times 10^7$	$8 \times 10^7$
22	$10^{10}$	$10^8$	$10^6$
23	$10^{10}$	$10^8$	$5 \times 10^6$
24	$10^{10}$	$10^8$	$8 \times 10^7$
25	$10^{10}$	$4 \times 10^9$	$10^6$
26	$10^{10}$	$4 \times 10^9$	$5 \times 10^6$
27	$10^{10}$	$4 \times 10^9$	$8 \times 10^7$

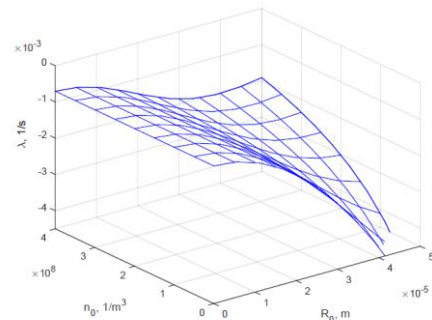


Figure 8. The decay rate by formula (2) for rows 5 of Tables III and IV.

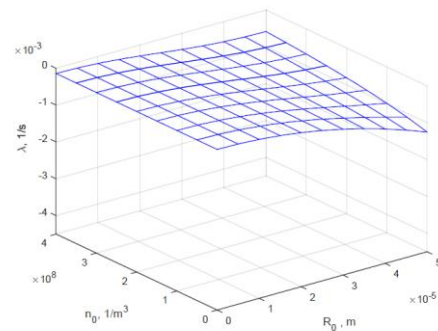


Figure 9. The decay rate by formula (2) for rows 17 of Table III and IV.

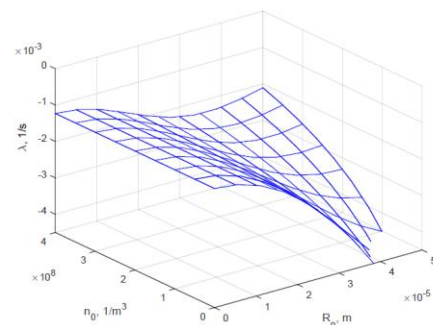


Figure 10. The decay rate by formula (2) for rows 25 of Table III and IV.

### III. VALIDITY SPACE

In this section we investigate the parametric space in terms of negative/positive  $\lambda$  (valid/invalid model). To present results in the form of 3D plots we choose two options: (a) vary  $E_i$  with  $M_i$  being fixed, (b) vary  $M_i$  with  $E_i$  being fixed. The points where  $\lambda$  is negative are displayed as 'o', the points where  $\lambda$  is positive are displayed as '\*'. The results are presented in Figs. 11-14.

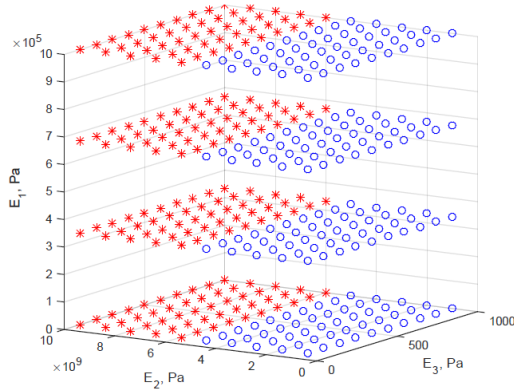


Figure 11. Valid and invalid points in the space of  $E_i$ .

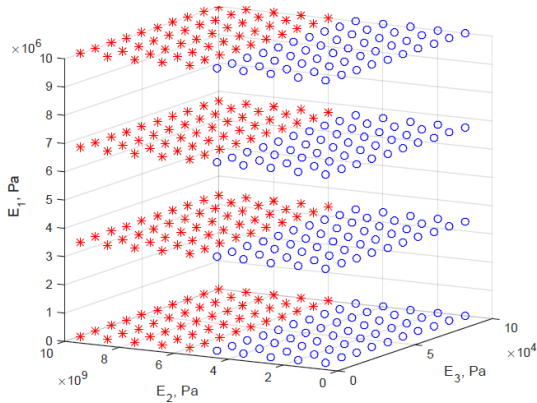


Figure 12. Valid and invalid points in the space of  $E_i$ .

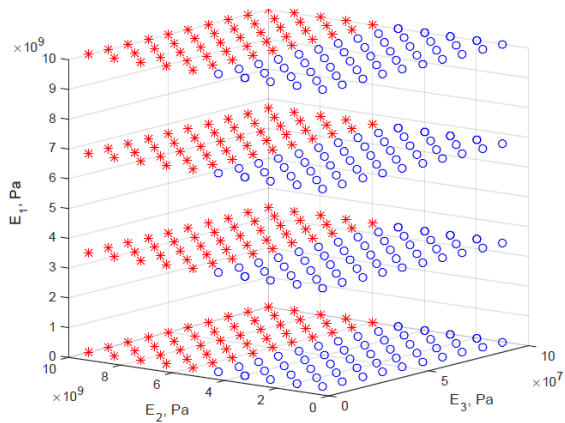


Figure 13. Valid and invalid points in the space of  $E_i$ .

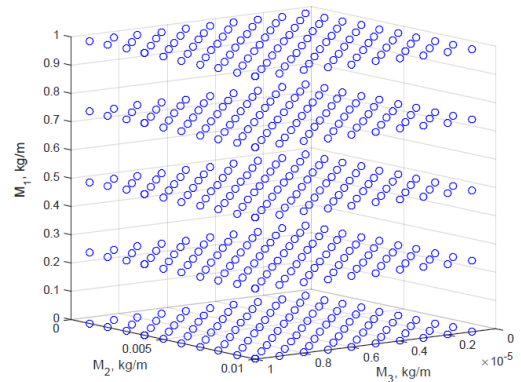


Figure 14. The validity area in the space of  $M_i$ .

See from Fig. 14 that all the points are valid points. Therefore, for different values of  $M_i$  the elastic wave is a *decaying* wave according to our model, which is a physically acceptable outcome.

### IV. CONCLUSIONS

We investigated the influence of the values of the rheological parameters on linear dynamics of elastic waves in porous media with fluid including gas bubbles. We evaluated the areas of validity of the decay rate of the wave in the parametric space.

#### CONFLICT OF INTEREST

The authors declare no conflict of interest.

#### AUTHOR CONTRIBUTIONS

Conceptualization, A.A and D.S.; Formal analysis, A. A.; Investigation, A.A and D.S.; Methodology, A.A.; Visualization, A.A. and D.S.; Writing—original draft, A.A.; Writing – review and editing, A.A and D.S.; all authors had approved the final version.

#### REFERENCES

- [1] M. Batzle, Z. Wang, "Seismic properties of pore fluids," *Geophysics*, vol. 57, no. 11, pp. 1396-408, Nov. 1992.
- [2] O. Kelder, D. M. Smeulders, "Observation of the Biot slow wave in water-saturated Nivelsteiner sandstone," *Geophysics*, vol. 62, no. 6, pp. 1794-6, Nov 1997.
- [3] O. Dazel, V. Tournat, "Nonlinear biot waves in porous media with application to unconsolidated granular media," *The Journal of the Acoustical Society of America*, vol. 127, no. 2, pp. 692-702, 2010 Feb.
- [4] T. M. Müller, B. Gurevich, M. Lebedev, "Seismic wave attenuation and dispersion resulting from wave-induced flow in porous rocks—A review," *Geophysics*, vol. 75, no. 5, 75A147-64, 2010 Sep 14.
- [5] H. Cheng, S. Luding, K. Saitoh, V. Magnanimo, "Elastic wave propagation in dry granular media: effects of probing characteristics and stress history," *International Journal of Solids and Structures*, May 8 2019.
- [6] A. Misra, N. NejadSadeghi, "Longitudinal and transverse elastic waves in 1D granular materials modeled as micromorphic continua," *Wave Motion*, May 21, 2019.
- [7] Y. F. Wang, J. W. Liang, A. L. Chen, Y. S. Wang, V. Laude, "Wave propagation in one-dimensional fluid-saturated porous metamaterials," *Physical Review B*, vol. 99, no. 13, 134304, 2019 Apr 16.

- [8] A. A. Ali, D. V. Strunin, "The role of rheology in modelling elastic waves with gas bubbles in granular fluid-saturated media," *Journal of Mechanics of Materials and Structures*, vol. 14, no. 1, pp. 1-24, 2019 Apr 7.
- [9] V. N. Nikolaevskiy, "Dynamics of viscoelastic media with internal oscillators," *In Recent Advances in Engineering Science*. Springer, Berlin, Heidelberg, 1989, pp. 210-221.
- [10] V. N. Nikolaevskiy, "Non-linear evolution of P-waves in visco-elastic granular saturated media," *Transport in Porous Media*; vol. 73, no. 2, p. 125, June 1 2008.
- [11] D. N. Mikhailov, "The influence of gas saturation and pore pressure on the characteristics of the Frenkel-Biot P waves in partially saturated porous media," *Izvestiya, Physics of the Solid Earth*. 2010 Oct 1; vol. 46, no. 10, pp. 897-909.
- [12] J. Joseph, G. Kuntikana, D. N. Singh, "Investigations on gas permeability in porous media," *Journal of Natural Gas Science and Engineering*, vol. 64, pp. 81-92, 2019 Apr 1.
- [13] V. N. Nikolaevskii, G. S. Stepanova, "Nonlinear seismic and the acoustic action on the oil recovery from an oil pool," *Acoustical Physics*. 2005 Dec 1; vol. 51, no. 1, S131-9.
- [14] V. N. Nikolaevskiy, D. V. Strunin, "The role of natural gases in seismic of hydrocarbon reservoirs," *Elastic Wave Effect on Fluid in Porous Media, Proceedings*, pp. 25-9, 2012.
- [15] V. N. Nikolaevskiy, "A real P-wave and its dependence on the presence of gas. *Izvestiya*," *Physics of the Solid Earth*, Jan 1, vol. 52, no. 1, pp.1-3, 2016.
- [16] S. Z. Dunin, D. N. Mikhailov, V. Nikolayevskii, "Longitudinal waves in partially saturated porous media: The effect of gas

bubbles," *Journal of applied mathematics and mechanics*. July 1, vol. 70, no. 2, pp. 251-63, 2006.

Copyright © 2020 by the authors. This is an open access article distributed under the Creative Commons Attribution License ([CC BY-NC-ND 4.0](https://creativecommons.org/licenses/by-nc-nd/4.0/)), which permits use, distribution and reproduction in any medium, provided that the article is properly cited, the use is non-commercial and no modifications or adaptations are made.

**Adham Ali** graduated from the University of Mosul (Department of Mathematics), Iraq, in 2000. He obtained his MSc degree from Tikrit University (Department of Mathematics), Iraq, in 2007, and PhD degree in Applied Mathematics from the University of Southern Queensland, Toowoomba, Australia, in 2019. He is currently a Lecturer at the Department of Mathematics, University of Kirkuk, Iraq.

**Dmitry Strunin** received his PhD from Moscow Institute of Physics and Technology, Russia, in 1983. He received his PhD from the Institute of Oceanology of the Russian Academy of Sciences, Moscow, Russia, in 1989. He has held researcher positions at the Universities of Melbourne and Wollongong, Australia, before joining the University of Southern Queensland (USQ), Toowoomba, Australia, in 1999. From 2009 he is an Associate Professor (Applied Mathematics) at the USQ. His research interests include dissipative systems, active chemical systems and nonlinear dynamics.